ELSEVIER

Polymer 44 (2003) 1449–1458

polymer

www.elsevier.com/locate/polymer

Amphiphilic cylindrical brushes with poly(acrylic acid) core and poly(*n*-butyl acrylate) shell and narrow length distribution

Mingfu Zhang[a], Thomas Breiner[b], Hideharu Mori[a], Axel H.E. Müller[a,c,*]

[a]*Makromolekulare Chemie II, Universität Bayreuth, NW II, D-95440 Bayreuth, Germany*
[b]*Makromolekulare Chemie I, Universität Bayreuth, D-95440 Bayreuth, Germany*
[c]*Bayreuther Zentrum für Kolloide und Grenzflächen, Universität Bayreuth, D-95440 Bayreuth, Germany*

Received 13 August 2002; accepted 25 October 2002

Abstract

Core–shell cylindrical polymer brushes with poly(*t*-butyl acrylate)-*b*-poly(*n*-butyl acrylate) (P*t*BA-*b*-P*n*BA) diblock copolymer side chains were synthesized via 'grafting from' technique using atom transfer radical polymerization (ATRP). The formation of well-defined brushes was confirmed by GPC and ^{1}H NMR. Multi-angle light scattering (MALS) measurements on brushes with 240 arms show that the radius of gyration scales with the degree of polymerization of the side chains with an exponent of 0.57 ± 0.05. The hydrolysis of the P*t*BA block of the side chains resulted amphiphilic cylindrical core–shell nanoparticles. In order to obtain a narrow length distribution of the brushes, the backbone, poly(2-hydroxyethyl methacrylate), was synthesized by anionic polymerization in addition to ATRP. The characteristic core–shell cylindrical structure of the brush was directly visualized on mica by scanning force microscopy (SFM). Brushes with 1500 block copolymer side chains and a length distribution of $l_w/l_n = 1.04$ at a total length $l_n = 179$ nm were obtained. By choosing the proper solvent in the dip-coating process on mica, the core and the shell can be visualized independently by SFM.

Keywords: Amphiphilic; Cylindrical brush; Core–shell nanoparticle

1. Introduction

It is well known that solution and bulk properties of polymer are dramatically influenced by their chain architecture. Cylindrical polymer brushes which have the same number of side chains as degree of polymerization of the main chain, are architecturally interesting for both experimental and theoretical chemists because of the possibility to form extended chain conformations, based on the intramolecular excluded-volume interactions between side chains densely grafted to the backbone. Since Tsukahara et al. [1,2] first succeeded in the synthesis of polymer brushes by radical polymerization of macromonomers, this type of polymers attracted considerable attention over the past years [3–20].

Generally, there are three methods to synthesize cylindrical polymer brushes. The first one, which was widely used in the past decade, is the conventional radical polymerization of macromonomers [1–8]. In this method, end-functionalized oligomers prepared by anionic polymerization are converted into polymerizable macromonomers, which form well-defined side chains of the brushes after subsequent radical polymerization. However, conventional radical polymerization of macromonomers normally yields a broad chain-length distribution of the resulting polymer. So the crude product may contain polymers with both star-like and brush-like shape in addition to residual macromonomers. It is worthy to note that living anionic polymerization [21] and living ring-opening metathesis polymerization (ROMP) [22–24] of macromonomers were also performed aiming to get well-defined polymacromonomer, however, high molecular weight polymers have not been prepared by these living polymerizations, so far. The second method is the 'grafting onto' technique [9–11]. The grafting of side chains onto a backbone was carried out via a coupling reaction. For example, coupling polystyryllithium with poly(chloroethyl vinyl ether) (PCEVE) resulted in a polymer brush with PCEVE as backbone and polystyrene (PS) as side chains [9,10]. However, insufficient grafting efficiency was often achieved using the grafting

* Corresponding author. Address: Makromolekulare Chemie II, Universität Bayreuth, NW II, D-95440 Bayreuth, Germany. Tel.: +49-921-553399; fax: +49-921-553393.
E-mail addresses: polymer-chem@uni-bayreuth.de, axel.mueller@uni-bayreuth.de (A.H.E. Müller).

0032-3861/03/$ - see front matter © 2003 Elsevier Science Ltd. All rights reserved.
PII: S0032-3861(02)00774-7

onto method. The last method, i.e. 'grafting from', appeared lately. In this method side chains of the brush are formed via atom transfer radical polymerization (ATRP) [25–27] initiated by the pendant initiating groups on the backbone [12,28,29]. By this method well-defined polymer brushes with high grafting density and rather narrow distributions of both backbone and side chains can be obtained, and the purification of resulting polymer brushes is much simpler comparing to the other two methods.

Cylindrical wormlike micelles have been investigated by many groups in recent years [30], most of them being formed by aggregation of surfactants. As an example, cetyltrimethylammonium bromide reversibly assembles into long, flexible wormlike micelles in 0.1 M KBr aqueous solution. These aggregates may dissociate or undergo structural changes under changed conditions. Similarly, block copolymers can form spherical or cylindrical micelles in selective solvents [31,32]. Although spheres are the most common morphology for block copolymer micelles, other types of supramolecular structures such as cylinders have also been found. For example, polyferrocenylsilane-*b*-poly[2-(*N*,*N*-dimethylamino)ethyl methacrylate] with a block ratio of 1:5 formed cylindrical micelles in aqueous solution [33]. In our case, the brushes with amphiphilic diblock copolymer (poly(acrylic acid)-*b*-poly(*n*-butyl acrylate), PAA-*b*-P*n*BA) side chains resemble the normal inverse block copolymer micelles in structure and therefore can be regarded as unimolecular wormlike micelles. Compared to block copolymer micelles they are very stable towards environmental changes since the side chains are covalently linked to the backbone. In addition, their length can be controlled in a much better way than for self-associating micelles. The ability of the hydrophilic PAA core of the amphiphilic core–shell brushes to coordinate with different metal cations can be used for the synthesis of novel nanosized organic/inorganic hybrids.

So far, there have been only a few reports about the synthesis of polymer brushes with amphiphilic side chains, whose peculiar topology makes them very attractive for applications involving unimolecular micelles [8,24]. Gnanou et al. [24] first reported the ROMP of norbornenoyl-endfunctionalized polystyrene-*b*-poly(ethylene oxide) macromonomers. Although complete conversion of macromonomer was achieved, the degree of polymerization was very low. Consequently, the polymacromonomer adopted a globular rather than a cylindrical shape. The difficulty in this method lies more in the synthesis of the macromonomer than in the polymerization. Later, Schmidt et al. [8] synthesized amphipolar cylindrical brushes with poly(2-vinylpyridine)-*b*-polystyrene side chains via radical polymerization of the corresponding block macromonomer. Similar polymer brushes with poly(α-methylstyrene)-*b*-poly(2-vinylpyridine) side chains were also synthesized by Ishizu via radical polymerization [34]. Again, the problem is the very wide length distribution of the obtained polymer brushes. To find an efficient and convenient methodology for the synthesis of well-defined amphiphilic cylindrical brushes still remains a challenge.

Very recently, we succeeded in the synthesis of the core–shell cylindrical brushes with amphiphilic block copolymer, poly(acrylic acid)-*b*-polystyrene (PAA-*b*-PS) or PS-*b*-PAA, as side chains by ATRP using the 'grafting from' technique [28]. Compared to the macromonomer route, this method is quite versatile and effective. ATRP is tolerant to many functionalities, so a multitude of monomers, including those with functional groups, can be polymerized to form the side chains. At the same time, the living character of ATRP enables the control of the distributions of backbone as well as side chains, so the resulting amphiphilic brushes have a well-defined structure.

As part of our continuous effort for the synthesis and applications of amphiphilic core–shell cylindrical brushes, we report here the synthesis and characterization of well-defined amphiphilic brushes with a PAA core and a soft P*n*BA shell. The chemical compatibility between the core and the shell of these brushes is somewhat better, compared to the amphiphilic brushes with PAA core and PS shell we synthesized before [28].

In the synthesis of cylindrical brushes with side chains containing PS block, we found that sometimes cross-linking occurred during the polymerization of styrene, probably due to intermolecular coupling reactions between spatially neighboring radical sites on the side chains. Using a high molar ratio of monomer to initiator and quenching the polymerization at quite low conversion of styrene ($<5\%$) we could suppress this undesirable side reaction [28]. Adding Cu(II) to decrease the radical concentration in ATRP and using 2,2′-bipyridine or its derivatives as ligands were also useful to avoid the coupling reaction, however, in this case the polymerization is very slow [29]. The polymerization of *n*-butyl acrylate (*n*BA) to form the shell can go to relatively high conversion (about 20%) without any cross-linking and the polymerization of *n*BA is quite fast under mild conditions.

In our previous syntheses [28] we prepared poly(2-hydroxyethyl methacrylate), poly(HEMA), which forms the backbone, via ATRP in ethanol. However, when aiming at high molecular weights this led to rather broad molecular weight distributions (MWDs) ($M_w/M_n < 1.4$). We now use an improved method to obtain more narrow MWD. In addition, anionic polymerization was also applied to synthesize poly(HEMA) with high molecular weight and very narrow distribution. Starting from this backbone, very uniform amphiphilic polymer brushes were obtained.

2. Experimental part

2.1. Materials

2-Hydroxyethyl methacrylate (HEMA, Acros, 96%) was

purified according to literature [35]. *t*-Butyl acrylate (*t*BA, BASF AG) was fractionated from CaH_2 at 45 mbar, stirred over CaH_2, degassed and distilled in high vacuum. *n*-Butyl acrylate (*n*BA, BASF AG) was vacuum distilled just before use. CuBr (95%, Aldrich) was purified by stirring overnight in acetic acid. After filtration it was washed with ethanol, diethyl ether, and then dried. 2,2′-Bipyridine (bpy) was recrystallized from ethanol to remove impurities. α-Bromoisobutyryl bromide and *N*,*N*,*N*′,*N*″,*N*″-pentamethyldiethylenetriamine (PMDETA) were purchased from Aldrich and used as received without further purification.

2-(Trimethylsilyloxy)ethyl methacrylate (TMS-HEMA, 97%, Aldrich) was purified according to the method described in the polymerization part. Trioctylaluminum (25 wt% in hexane, Aldrich) and *sec*-butyllithium (*sec*-BuLi, 1.3 M in cyclohexane, Aldrich) were used without further purification. 1,1-Diphenylethylene (DPE, 97%, Aldrich) was vacuum distilled and dried by adding a small amount of *sec*-BuLi solution until the color changed to light yellow. Lithium chloride (LiCl, >98%, Fluka) was dried at 300 °C under vacuum overnight, and then dissolved in THF. THF (p.a., Merck) was purified first by distillation under nitrogen from CaH_2 and then by refluxing over potassium.

2.2. Synthesis of poly(2-hydroxyethyl methacrylate), poly(HEMA)

(a) *via anionic polymerization* [36,37]. The silyl-protected monomer (2-(trimethylsilyloxy)ethyl methacrylate, TMS-HEMA) was purified on a vacuum line using home-made glassware consisting of two flasks connected by a glass bridge. Into one flask 50 ml of TMS-HEMA were added and degassed by three freeze-pump-thaw cycles. A small amount of trioctylaluminium solution (in hexane) was added until the color changed to light yellow, indicating the complete removal of water. The monomer was then frozen by liquid N_2 and evacuated. During thawing, hexane evaporated and was caught in the cooling trap of vacuum line. Now the second flask was cooled with liquid N_2 and the monomer was condensed into this flask under gentle heating. After thawing the monomer was transferred into the reactor with a syringe equipped with a stainless steel needle (dry, flush with N_2). For the anionic polymerization, 300 ml of THF were placed into the reactor and cooled down to −75 °C. Then LiCl solution (in THF, tenfold molar excess with respect to the initiator used) was added. After the system changed to a light red color (indicating absence of water) by adding a small amount of *sec*-BuLi solution, the calculated amount of *sec*-BuLi was added via a syringe. Then, a fourfold molar excess of DPE (with respect to the amount of *sec*-BuLi) was placed into the reactor. Ten minutes later, when the formation of the 1,1-diphenyl-3-methylpentyl-lithium initiator species was completed, the monomer was added. The polymerization proceeded for 2.5 h at −75 °C and finally was terminated by adding 1 ml of a well degassed methanol/acetic acid (10/1) mixture. After the polymerization THF was removed by rotating evaporation. The resulting polymer was dissolved in methanol and precipitated in water mixed with several drops of HCl solution (32%). The final deprotected product, poly(HEMA), was freeze-dried from dioxane. ^{1}H NMR (CD_3OD): $\delta = 4.04$ ($-CH_2-OCO$), 3.77 ($-CH_2-OH$), 2.20–1.40 ($-CH_2-C$), 1.30–0.70 ($-CH_3$) ppm.

(b) *via ATRP*. Poly(HEMA) was prepared in mixture solvent of methylethyl ketone and 1-propanol (v/v = 7/3) by ATRP using CuCl/2,2′-bipyridine as catalyst, according to literature [35].

2.3. Preparation of poly(2-(2-bromoisobutyryloxy)ethyl methacrylate (PBIEM)

The procedure of the synthesis of PBIEM detailed in our previous paper [28]. ^{1}H NMR ($CDCl_3$): $\delta = 4.37$, 4.21 ($-CH_2-OCO$), 2.20–1.40 ($-CH_2-C$), 1.97 [$-C(Br)(CH_3)_2$], 1.30–0.70 ($-CH_3$) ppm.

2.4. Typical ATRP procedure for the synthesis of brushes [25–27]

All operations except the polymerization were carried out in glove box under nitrogen atmosphere. CuBr (or CuCl), initiator, monomer, acetone (which was added in some cases) and decane (internal standard, 1/10 molar ratio relative to monomer) were added into a round flask. The mixture was stirred until all the initiator was dissolved completely. Then an initial sample was taken for gas chromatography (GC) measurement and finally the ligand, PMDETA, was added. The flask was then sealed and immersed in an oil bath at a preset temperature for a certain time. The polymerization was stopped by cooling to room temperature and exposed the reaction mixture to air. After polymerization, the catalyst was removed by an adsorption filtration through an alumina column and the resulting polymer was precipitated from chloroform into mixture of methanol and water (v/v = 4/1 to 3/1). The produced polymer was dissolved in benzene and freeze-dried. For the synthesis of polymer brushes with diblock copolymer side chains, the purified brush polymers with homopolymer side chains were used as initiators.

2.5. Hydrolysis of the poly(t-butyl acrylate) blocks [38]

The brush was dissolved in CH_2Cl_2 and then a fivefold molar excess of CF_3COOH (with respect to the amount of the *t*-butyl group in the brush) was added. The reaction mixture was stirred at room temperature for 24 h. During the hydrolysis, the resulting brush with PAA-*b*-P*n*BA side chains precipitated in CH_2Cl_2 gradually. Finally, solvent and CF_3COOH were removed by rotating evaporation followed by freeze-drying. Traces of CF_3COOH in the polymer were removed by vacuum drying at 40 °C overnight.

2.6. Analysis

Monomer conversion was determined by GC from the concentration of residual monomer with decane as an internal standard, using a polymethylsiloxane capillary column. Proton nuclear magnetic resonance (^{1}H NMR) spectra were recorded with a Bruker AC-250 spectrometer at room temperature in $CDCl_3$ or CD_3OD (or mixture of them). The apparent molecular weights of the brushes were measured by gel permeation chromatography (GPC) using THF as eluent at a flow rate of 1.0 ml/min at room temperature. Column set: 5μ SDV gel, 10^5, 10^4, 10^3, 10^2 Å, 30 cm each (PSS, Germany); detectors: Waters 410 differential refractometer and Waters photodiode array detector operated at 254 nm. PS standards (PSS) were used for the calibration of the column set. The samples for scanning force microscopy (SFM) measurements were prepared by dip-coating from dilute solutions of brushes in different solvents, with concentration of 10^{-6}–10^{-4} g/ml, onto freshly cleaved mica surface. The SFM images were taken with a Digital Instruments Dimension 3100 microscope operated in Tapping Mode (free amplitude of the cantilever ≈30 nm, set point ratio ≈0.98).

Membrane osmometry was performed in toluene at 35 °C in order to determine the true number-average molecular weight of the polyinitiator (forming the backbone) using a cellulose triacetate membrane with a Gonotec Osmomat 090 (Gonotec GmbH, Germany). GPC with a multi-angle light scattering detector (GPC-MALS) was used to determine the absolute molecular weights of the brushes. THF was used as eluent at a flow rate of 1.0 ml/min. Column: 30 cm linear SDV 5μ (PSS); detectors: DAWN DSP-F MALS and PSS ScanRef interferometer, both equipped with 632.8 nm He–Ne laser. The ScanRef interferometer was also used to measure refractive index increment (d*n*/d*c*) in the offline mode.

Dynamic light scattering (DLS) was performed on an ALV DLS/SLS-SP 5022F compact goniometer system with an ALV 5000/E correlator and a He–Ne laser ($\lambda = 632.8$ nm). Prior to the light scattering measurements the sample solutions were filtered using Millipore Teflon filters with a pore size of 0.45 μm.

3. Results and discussion

The synthetic route for amphiphilic cylindrical brushes with PAA core and P*n*BA shell is shown in Scheme 1.

3.1. Synthesis of polyinitiator (poly(2-(2-bromoisobutyryloxy)ethyl methacrylate, PBIEM)

Obviously the length distribution of the cylindrical polymer brushes is only dependent on the molecular weight distribution (MWD) of the backbone, which is the polyinitiator (PBIEM) in our case. Thus, the synthesis of a polyinitiator with a narrow MWD is crucial to get uniform cylinders. Although ATRP can give quite good control on the polymerization of many monomers, normally anionic polymerization is still the better choice to obtain polymer with very narrow MWD, despite of its strict purification procedure for monomer, solvents and all additives. In order to protect the reactive hydroxy group of HEMA, trimethylsilyl-protected HEMA (TMS-HEMA) was used as monomer, since it is very easy to remove the trimethylsilyl groups of the produced polymer. For comparison, ATRP was also carried out to synthesize poly(HEMA).

The limited solubility of poly(HEMA) in THF and its adsorption to the column material prevent the direct analysis of the MWD under standard conditions of GPC. However, after esterification of poly(HEMA) with α-bromoisobutyryl bromide, the polyinitiator PBIEM was obtained which is THF-soluble. Complete esterification of the hydroxy groups of poly(HEMA) was confirmed by ^{1}H NMR (Fig. 5(A)). GPC measurements clearly show that the polyinitiator obtained via anionic polymerization has a more narrow MWD than that from ATRP, as shown in Table 1 and Fig. 1. In addition, much higher molecular weight of poly(HEMA) can be achieved by anionic polymerization. It is worth to mention that a small peak with double molecular weight was observed in the GPC trace of PBIEM-II synthesized via anionic polymerization (shown in Fig. 1), indicating that probably some side reactions during the termination of the living polymer chain occurred. This has been attributed to an attack of the anionic chain end on the TMS group [37]. Nevertheless, the amount of the polymer with double

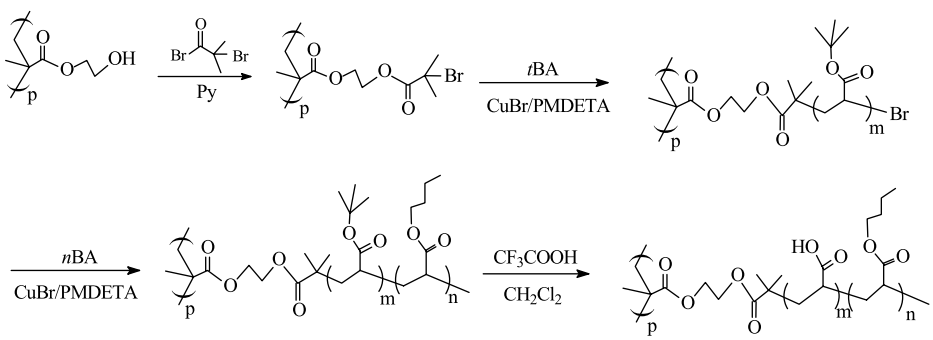

Scheme 1. Synthetic procedure for amphiphilic core–shell cylindrical brushes.

Table 1
Characterization of polyinitiators, poly(2-(2-bromoisobutyryloxy)ethyl methacrylate) (PBIEM), synthesized via different polymerization methods

Code	Polymerization method	$10^{-4} \times M_{n,GPC}$	$10^{-4} \times M_{n,osm.}$ [a]	PDI_{GPC}	$DP_{n,osm.}$
PBIEM-I	ATRP	2.05	6.68	1.16	240
PBIEM-II	Anionic polymerization	8.01	41.82	1.08	1500

[a] Obtained by membrane osmometry.

molecular weight is very small (1.3 mol%) and the polydispersity of the PBIEM-II is very low (PDI = 1.08).

Since the polyinitiator will form the backbone of the brush, the knowledge of its true molecular weight (or degree of polymerization) is very important for the further characterization of the brushes. Thus, membrane osmometry was used here to determine the true number-average molecular weights of polyinitiators. The results are shown in Table 1. The number-average molecular weights of the two polyinitiators are 6.68×10^4 and 4.18×10^5, respectively, corresponding to number-average degrees of polymerization $DP_n = 240$ and 1500, respectively. By using these two polyinitiators, amphiphilic cylindrical brushes with different backbone lengths were obtained. The reduced osmotic pressure, Π/c, of the polyinitiator solution in toluene at 35 °C was almost constant in the concentration range from 1 to 13 g/l, which indicates the membrane osmometry measurements of polyinitiators were done near θ condition.

3.2. Synthesis of cylindrical brushes with P*t*BA core and P*n*BA shell

Tables 2 and 3 present the results of ATRP by using two different polyinitiators. Well-defined polymer brushes with homopolymer and diblock copolymer side chains were obtained, as confirmed by the monomodal GPC eluograms (Figs. 2 and 3). The MWDs of the resulting brushes are quite low in most cases (PDI < 1.3), indicating that intermacromolecular coupling reactions during the polymerization are negligible. The polymerizations of both *t*BA and *n*BA are fast and can go to relatively high conversion without the occurrence of cross-linking. In the case of the polymerization of *n*BA, the reaction system became very viscous at the final stage of polymerization, but coupling reaction was not observed. Contrarily, when styrene was used as monomer to form the polymer shell instead of *n*BA, cross-linking happened very often at quite low monomer conversion when the brush backbone was long (using PBIEM-II as polyinitiator), although different polymerization conditions (such as ligand type, monomer/initiator ratio, and solvent addition) were tried.

It has to be pointed out that since the polyinitiator and poly(macroinitiator) (i.e. the brushes with P*t*BA side chains) are solids, the polymerization mixture (catalyst, initiator, monomer, internal standard, and solvent) had to be stirred until all initiator was completely dissolved before starting the polymerization by adding ligand and placing the flask into an oil bath. Especially the polyinitiator with high molecular weight (PBIEM-II) dissolves in monomer (*t*BA) much slower than PBIEM-I. Thus, if the time of stirring before the addition of ligand is not long enough (which means the polyinitiator is incompletely dissolved), the MWD of the final product will be somehow broader (such as

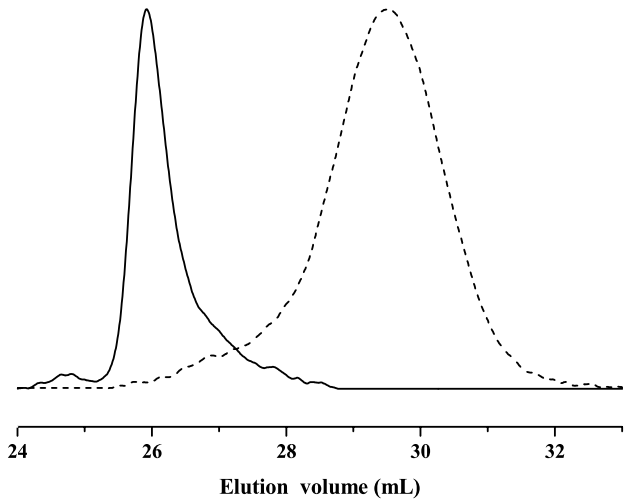

Fig. 1. GPC traces of two polyinitiators: (– –) PBIEM-I (ATRP); (—) PBIEM-II (anionic polymerization).

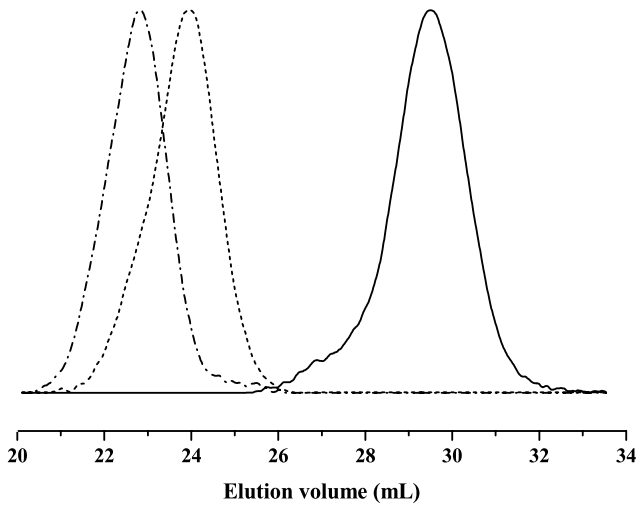

Fig. 2. GPC traces of PBIEM-I ($DP_n = 240$) and the corresponding short brushes with homopolymer and diblock copolymer side chains (—: PBIEM-I; – –: Brush with P*t*BA side chains (Brush 5, $[(t\,BA)_{34}]_{240}$); –·–: Brush with P*t*BA-*b*-P*n*BA side chains (Brush 6, $[(t\,BA)_{34}$-*b*-$(n\,BA)_{71}]_{240}$).

Table 2
Synthesis and characterization of short cylindrical brushes via ATRP using PBIEM-I as polyinitiator

Brush	Initiator	Monomer	[CuX]/[PMDETA]/[Br][a]/[M]	T (°C)	Time (min)	Conv. (%)	$10^{-5} \times M_{n,GPC}$[b]	PDI[b]	$10^{-6} \times M_{n,MALS}$	R_g (nm)	$DP_{sc,LS}$[c]
1	PBIEM-I	*t*BA	1[d]/2/1/200	50	20	29.3	2.98	1.17	1.44	16.3	45
2	PBIEM-I	*t*BA	1[e]/1/1/250	50	30	10.8	2.07	1.15	0.93	11.6	28
3	PBIEM-I	*t*BA	1[d]/2/1/250	50	20	22.8	2.95	1.16	1.25	16.0	39
4	Brush 3	*n*BA	3.2[d]/6.1/1[f]/890	70	65	18.1	5.55	1.25	4.90	33.5	157
5	PBIEM-I	*t*BA	0.5[e]/0.5/1/300	50	35	12.2	2.41	1.17	1.12	12.9	34
6	Brush 5	*n*BA	1.6[e]/3.2/1[f]/520	70	85	9.1	3.65	1.27	3.29	23.4	105

[a] Molar concentration of initiating bromine groups in PBIEM or polymer brush with P*t*BA side chains.
[b] Calibrated against linear PS standards.
[c] Degree of polymerization of the side chain, calculated from $M_{n,MALS}$.
[d] CuCl.
[e] CuBr.
[f] Calculated from $M_{n,MALS}$.

Brush 7 in Table 3), because in this case not all the polyinitiator molecules start the polymerization at the same time. After the formation of P*t*BA side chains, the molecular weights of the resulting brushes are very high, and correspondingly their solubility in the second monomer (*n*BA) decreases. In order to dissolve these brushes, adding suitable solvent such as acetone is helpful. As shown in Table 3 (Brush 10) and Fig. 3, a core–shell brush with more narrow MWD was obtained after adding 30 vol% acetone.

Obviously, the molecular weights of these brushes obtained from GPC against linear PS standards are just the apparent ones. The absolute molecular weights as well as the radii of gyration, R_g, in THF of these brushes were determined by GPC-MALS. With the same backbone but longer side chain length, R_g of the brushes increase with a scaling law $R_g \propto DP_{sc}^{0.57\pm0.05}$, as shown in Fig. 4. To our best knowledge this is the first experimental quantitative investigation about the influence of side chain length on radius of gyration of the cylindrical brushes with exactly identical backbone length. Further systematic study on this relationship is needed since only a few data points are available at the moment. Nevertheless, polymer brushes synthesized via grafting from method are the best candidates to study the independent influence of side chain length on overall dimensions of the brushes, because the length of backbone is fixed. On the other hand, polymacromonomer method is suitable for the investigation of the relationship between the radius of gyration and the backbone DP since here the side chain DP is fixed and a broad MWD of backbone is obtained. Using GPC-MALS coupling such measurements were performed by Schmidt et al. [3,4]. It is expected that the main chain stiffness of the polymer brush increases with increasing side chain length, because the stronger overcrowding of longer side chains forces the otherwise flexible main chain into a more stretched conformation.

Fig. 5 shows the ^{1}H NMR spectra of polyinitiator as well as brushes. In Fig. 5(A), there are two typical peaks at 4.21 and 4.37 ppm (a and a'), which represent the methylene protons between two ester groups of the polyinitiator. There is no peak at 3.77 ppm, which is assigned to methylene protons adjacent to the hydroxy group in poly(HEMA), indicating the complete esterification of poly(HEMA) with 2-bromoisobutyryl bromide. After the formation of the brush with P*t*BA side chains, a characteristic strong peak at 1.44 ppm (peak c) corresponding to methyl protons in *t*-butyl group ($-C(CH_3)_3$) appears, as shown in Fig. 5(B). The successful formation of the core–shell brush with P*n*BA shell is confirmed by the appearance of several new peaks in Fig. 5(C), such as the typical triple peak at 0.94 ppm and the peak at 4.04 ppm, corresponding to the terminal methyl protons ($-O(CH_2)_3CH_3$) and the methylene protons adjacent to oxygen ($-OCH_2(CH_2)_2CH_3$) in the *n*-butyl group, respectively. The protons from the other two methylene

Table 3
Synthesis and characterization of long cylindrical brushes via ATRP using PBIEM-II as polyinitiator

Brush	Initiator	Momomer	[CuBC]/[PMDETA]/[Br][a]/[M]	T (°C)	Time (min)	Conv. (%)	$10^{-5} \times M_{n,GPC}$	PDI[b]	$10^{-6} \times M_{n,MALS}$	R_g (nm)	$DP_{sc,LS}$[c]
7	PBIEM-II	*t*BA	0.5/0.5/1/300	50	35	10.0	6.83	1.31	7.57	51.6	37
8	Brush 7	*n*BA	1.9/3.9/1[d]/575	70	75	7.0	7.72	1.40	22.16	81.3	113
9	PBIEM-II	*t*BA	0.5/0.5/1/300	50	40	12.5	7.37	1.18	6.69	50.2	33
10[e]	Brush 9	*n*BA	2.3/2.4/1[d]/505	70	60	9.3	8.85	1.34	–	–	77[f]

[a–d] see Table 2.
[e] Adding 30 vol% of acetone.
[f] Calculated according to ^{1}H NMR.

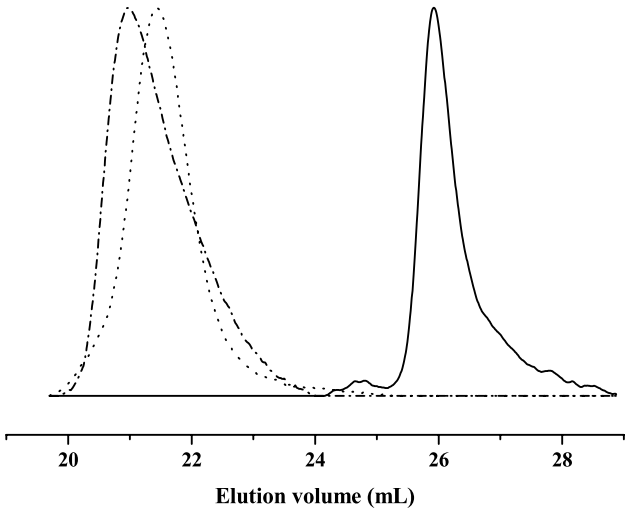

Fig. 3. GPC traces of PBIEM-II ($DP_n = 1500$) and the corresponding long brushes with homopolymer and diblock copolymer side chains (—: PBIEM-II; – –: Brush with P*t*BA side chains (Brush 9, $[(t\text{BA})_{33}]_{1500}$); –·–: Brush with P*t*BA-*b*-P*n*BA side chains (Brush 10, $[(t\text{BA})_{33}$-*b*-$(n\text{BA})_{44}]_{1500}$).

groups in the *n*-butyl group can also be seen at 1.35 ppm (overlapped with protons from the *t*-butyl group) and 1.60 ppm.

3.3. Formation of amphiphilic core–shell cylindrical brushes

By selective hydrolysis of the P*t*BA block of the side chains, amphiphilic core–shell cylindrical brushes with poly(acrylic acid) core and P*n*BA shell were obtained. The hydrolysis procedure was very simple and effective. As shown in Fig. 6, the disappearance of the characteristic strong peak at 1.44 ppm corresponding to the methyl protons of the *t*-butyl group demonstrates the successful hydrolysis of P*t*BA block of the side chains. The resulting

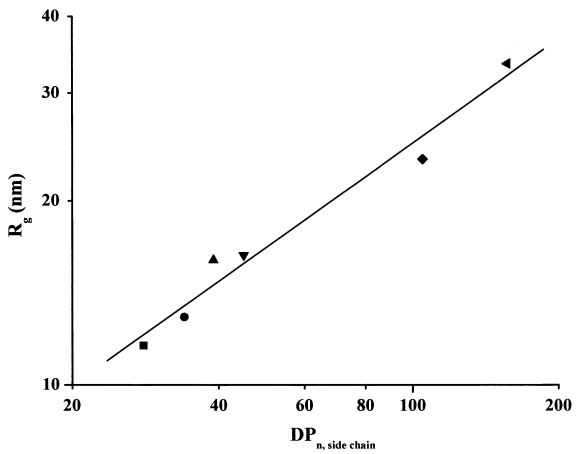

Fig. 4. Radius of gyration versus DP of side chain of the brushes with PBIEM-I as backbone (■: Brush 2; ●: Brush 5; ▲: Brush 3; ▼: Brush 1; ◆: Brush 6; ◄: Brush 4).

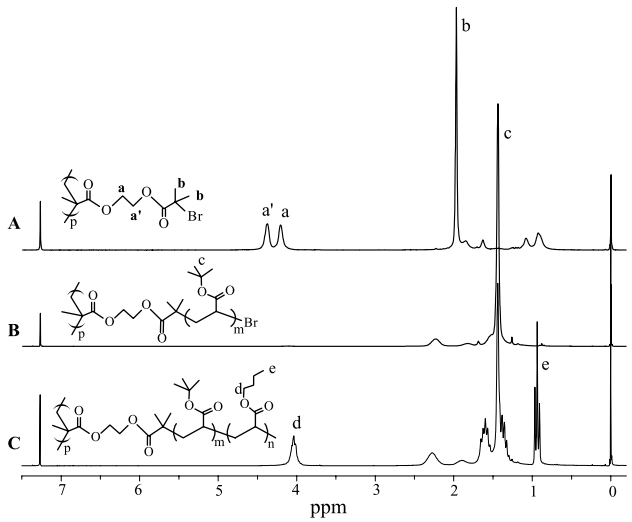

Fig. 5. ^{1}H NMR spectra of (A) polyinitiator (PBIEM-I); (B) brushes with P*t*BA homopolymer side chains ($[(t\text{BA})_{34}]_{240}$, Brush 5); and (C) brushes with P*t*BA-*b*-P*n*BA diblock copolymer side chains ($[(t\text{BA})_{34}$-*b*-$(n\text{BA})_{71}]_{240}$, Brush 6).

brushes resemble inverse cylindrical micelles of amphiphilic block copolymers in nonpolar solvents. By simply changing the type and quality of solvents, one can easily adjust the sizes of the core and the shell of these amphiphilic brushes.

DLS was used to characterize the amphiphilic core–shell brushes in dilute THF solution. Fig. 7(A) shows the typical normalized field correlation functions of a long amphiphilic core–shell brush (hydrolysis product of Brush 8) at room temperature. The CONTIN [39] analysis of these autocorrelation functions shows a monomodal decay time distribution at all scattering angles. Apparent hydrodynamic radii of the amphiphilic brushes were calculated according to Stokes–Einstein equation under the assumption that the scattering particles behave as hard spheres. Fig. 7(B) shows the hydrodynamic radius distribution of this amphiphilic brush in THF at scattering angle of 30°. The *z*-average hydrodynamic radius of this brush at 30° is 72.4 nm.

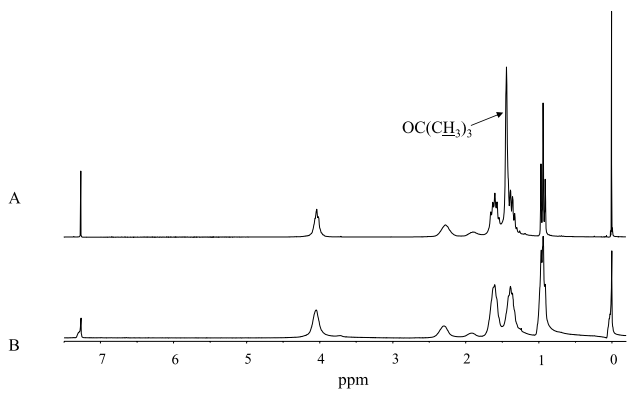

Fig. 6. ^{1}H NMR spectra of core–shell brushes (A) Brush 6, $[(t\text{BA})_{34}$-*b*-$(n\text{BA})_{71}]_{240}$; and (B) the hydrolysis product of Brush 6, $[(\text{AA})_{34}$-*b*-$(n\text{BA})_{71}]_{240}$.

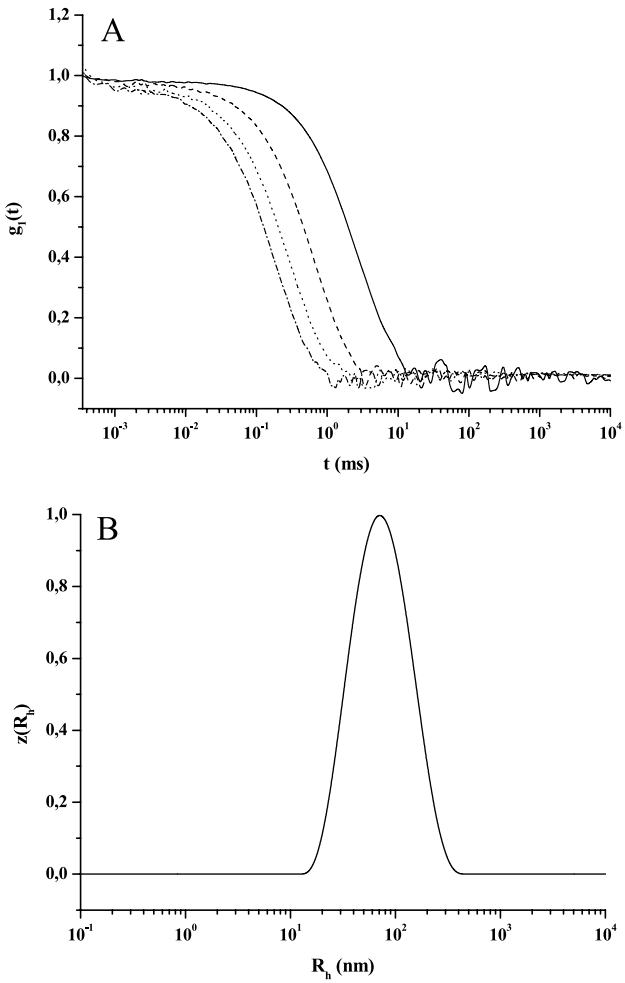

Fig. 7. (A) Normalized field correlation of the hydrolysis product of Brush 8, $[(AA)_{37}$-*b*-$(n\,BA)_{76}]_{1500}$, in THF ($c = 1.0$ g/l) at different angles (—: 30°; – –: 60°; - - -: 90°; –·–: 120°); (B) The corresponding hydrodynamic radius distribution of this brush at 30°.

3.4. Scanning force microscopy characterization of cylindrical brushes

The core–shell brushes were further characterized by SFM in order to visualize the unimolecular cylinders. All samples for SFM were prepared by dip-coating from dilute solutions using freshly cleaved mica as substrate.

Fig. 8 shows the SFM images of one amphiphilic brush $[(AA)_{39}$-*b*-$(n\,BA)_{118}]_{240}$ (hydrolysis product of Brush 4), dip-coated from 1-butanol on mica. From SFM images this polymer appears starlike rather than brushlike, because of its very long side chains and somewhat short backbone. From the phase image one can easily observe a core with a surrounding corona. In the case of the brushes with PAA-*b*-PS side chains we did not see this apparent phase difference from SFM images [28]. Similar SFM images were also found for the cylindrical brush with P*n*BA core and PS shell, and the driving force was claimed to be the collapse of the PS block on mica (because the nonpolar PS block has weak interaction with the polar substrate mica) [29]. However, for the amphiphilic brush $[(AA)_{39}$-*b*-$(n\,BA)_{118}]_{240}$, both PAA and P*n*BA have attractive interactions with mica, therefore the core as well as the shell of this brush should be tightly absorbed to the substrate. Thus, we conclude that the core shown in the SFM images corresponds to PAA and the backbone of the brush, whereas the corona corresponds to the P*n*BA shell. This apparent phase difference stems from the large difference of stiffness between PAA and P*n*BA, taking into account that the glass transition temperature of P*n*BA is much lower than that of PAA (and also P*t*BA).

In order to obtain polymers exhibiting cylindrical shape, one has to increase the aspect ratio, corresponding to the ratio between the backbone and the side chains lengths. Fig. 9 shows SFM images of another core–shell brush $[(t\,BA)_{34}$-*b*-$(n\,BA)_{71}]_{240}$ (Brush 6), with exactly the same backbone as the above brush but shorter side chains on a mica surface. The polymer cylinders are directly visualized. One can clearly observe some millipede-like structures, especially in the phase image. The cross-section analysis of the cylinder marked with a rectangle shows that its height (2.5 ± 0.2 nm) is much smaller than its diameter (20 ± 2 nm, neglecting the length of hairs), indicating a strong deformation of the cylindrical profile on mica. This is due to the attractive interaction between the side chains and the substrate. The length distribution of the polymer

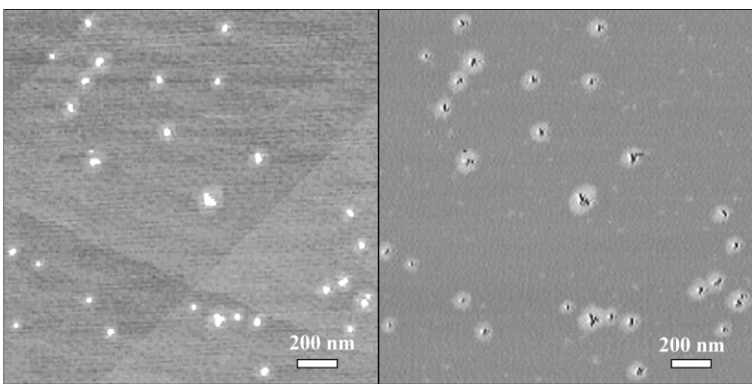

Fig. 8. SFM Tapping Mode images of the amphiphilic brush $[(AA)_{39}$-*b*-$(n\,BA)_{118}]_{240}$ (hydrolysis product of Brush 4), dip coated from dilute 1-butanol solution on mica: (left) height image (z-range: 5 nm) and (right) phase image (range: 30°).

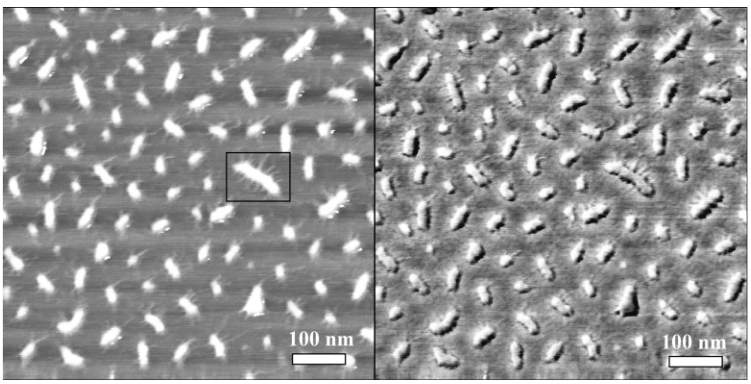

Fig. 9. SFM Tapping Mode images of the brush $[(t\,BA)_{34}$-b-$(n\,BA)_{71}]_{240}$ (Brush 6), dip coated from dilute THF solution on mica: (left) height image (z-range: 5 nm) and (right) phase image (range: 30°).

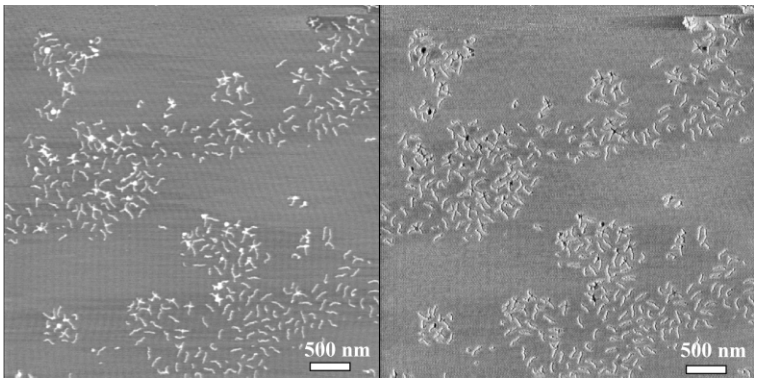

Fig. 10. SFM Tapping Mode images of the brush, $[(AA)_{37}$-b-$(n\,BA)_{76}]_{1500}$ (hydrolysis product of Brush 8) dip coated from dilute $CH_3OH/CHCl_3$ (4/1) solution on mica: (left) height image (z-range: 7 nm) and (right) phase image (range: 10°).

cylinders in Fig. 9 is somehow broad, although the MWD of the polyinitiator (PBIEM-I) for these cylinders is not very high (PDI = 1.16). This also indicates the necessity of synthesizing polyinitiators with very narrow distribution in order to get uniform polymer cylinders.

When using the polyinitiator synthesized via anionic polymerization (PBIEM-II), long amphiphilic core–shell cylinders with much more narrow backbone length distribution were obtained. Fig. 10 shows the SFM images of the amphiphilic brush $[(AA)_{37}$-b-$(n\,BA)_{76}]_{1500}$ (hydrolysis product of Brush 8). The high uniformity as well as the regular cylindrical shape of the polymer cylinders enables us to perform a statistical analysis. The number-average and weight-average lengths of 249 individual cylinders in Fig. 10 (neglecting those cylinders which overlap) are $l_n = 179$ nm and $l_w = 186$ nm, respectively, with a polydispersity $l_w/l_n = 1.04$ which agrees well with the polydispersity of the backbone ($M_w/M_n = 1.08$).

Since the DP of the backbone is 1500 and the number-average length obtained from SFM image is 179 nm for the brush $[(AA)_{37}$-b-$(n\,BA)_{76}]_{1500}$, the length per monomer unit of the backbone is calculated to be $l_{unit} = 0.12$ nm. This

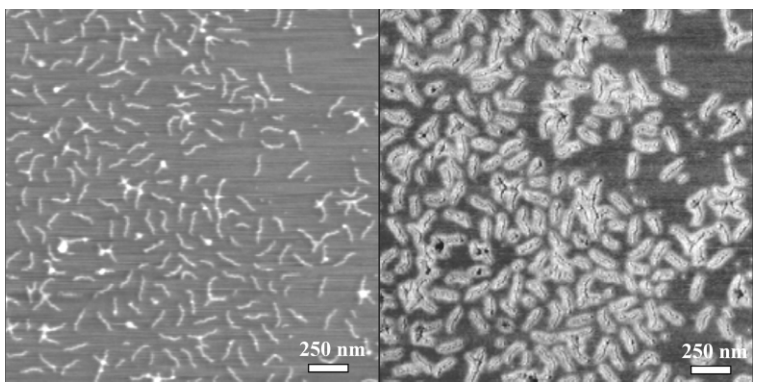

Fig. 11. SFM Tapping Mode images of the brush, $[(AA)_{37}$-b-$(n\,BA)_{76}]_{1500}$ (hydrolysis product of Brush 8) dip coated from dilute $CH_3OH/CHCl_3$ (1/1) solution on mica: (left) height image (z-range: 6 nm) and (right) phase image (range: 40°).

value is lower than $l_{unit} = 0.25$ nm for the all-*trans* conformation of an aliphatic chain, but it is comparable to that of the brush with poly(methyl acrylate) main chain and poly(methyl methacrylate) side chain [15].

The phase difference between the core and the shell is not very clear in Fig. 10, probably because the shell (P*n*BA) is not well extended in the mixture of methanol and chloroform with volume ratio of 4/1. However, the phase difference is enhanced dramatically when the ratio of the two solvents was changed to 1/1, as shown in Fig. 11. In the height image the corona is invisible, probably because the height of the P*n*BA shell is too small to be detectable. However, in the phase image the corona is very clear, making it possible to obtain size information about the core and the shell directly from the SFM height and phase images, respectively. For example, the average diameter of the core of cylinders in Fig. 11 is measured to be about 25 nm and the diameter of whole cylinder (core and shell) is about 65 nm.

Acknowledgements

This work was supported by the Deutsche Forschungsgemeinschaft. We want to thank A. Krökel for the osmotic pressure measurements.

References

[1] Tsukahara Y, Mizuno K, Segawa A, Yamashita Y. Macromolecules 1989;22:1546.
[2] Tsukahara Y, Tsutsumi K, Yamashita Y, Shimada S. Macromolecules 1990;23:5201.
[3] Wintermantel M, Schmidt M, Tsukahara Y, Kajiwara K, Kohjiya S. Macromol Rapid Commun 1994;15:279.
[4] Wintermantel M, Gerle M, Fischer K, Schmidt M, Wataoka I, Urakawa H, Kajiwara K, Tsukahara Y. Macromolecules 1996;29:978.
[5] Sheiko SS, Gerle M, Fischer K, Schmidt M, Möller M. Langmuir 1997;13:5368.
[6] Dziezok P, Sheiko SS, Fischer K, Schmidt M, Möller M. Angew Chem, Int Ed Engl 1997;36:2812.
[7] Kawaguchi S, Akaike K, Zhang ZM, Matsumoto H, Ito K. Polym J 1998;30:1004.
[8] Djalali R, Hugenberg N, Fischer K, Schmidt M. Macromol Rapid Commun 1999;20:444.
[9] Schappacher M, Billaud C, Paulo C, Deffieux A. Macromol Chem Phys 1999;200:2377.
[10] Deffieux A, Schappacher M. Macromolecules 1999;32:1797.
[11] Ryu SW, Hirao A. Macromolecules 2000;33:4765.
[12] Beers KL, Gaynor SG, Matyjaszewski K, Sheiko SS, Möller M. Macromolecules 1998;31:9413.
[13] Nemoto N, Nagai M, Koike A, Okada S. Macromolecules 1995;28:3854.
[14] Wataoka I, Urakawa H, Kajiwara K, Schmidt M, Wintermantel M. Polym Int 1997;44:365.
[15] Gerle M, Fischer K, Roos S, Müller AHE, Schmidt M, Sheiko SS, Prokhorova S, Möller M. Macromolecules 1999;32:2629.
[16] Terao K, Takeo Y, Tazaki M, Nakamura Y, Norisuye T. Polym J 1999;31:193.
[17] Terao K, Nakamura Y, Norisuye T. Macromolecules 1999;32:711.
[18] Rouault Y. Macromol Theory Simul 1998;7:359.
[19] Saariaho M, Subbotin A, Ikkala O, ten Brinke G. Macromol Rapid Commun 2000;21:110.
[20] Subbotin A, Saariaho M, Stepanyan R, Ikkala O, ten Brinke G. Macromolecules 2000;33:6168.
[21] Tsukahara Y, Inoue J, Ohta Y, Kohjiya S, Okamoto Y. Polym J 1994;26:1013.
[22] Feast WJ, Gibson VC, Johnson AF, Khosravi E, Mohsin MA. Polymer 1994;35:3542.
[23] Heroguez V, Breunig S, Gnanou Y, Fontanille M. Macromolecules 1996;29:4459.
[24] Heroguez V, Gnanou Y, Fontanille M. Macromolecules 1997;30:4791.
[25] Wang JS, Matyjaszewski K. J Am Chem Soc 1995;117:5614.
[26] Kotani Y, Kato M, Kamigaito M, Sawamoto M. Macromolecules 1996;29:6979.
[27] Matyjaszewski K, Xia J. Chem Rev 2001;101:2921.
[28] Cheng G, Böker A, Zhang M, Krausch G, Müller AHE. Macromolecules 2001;34:6883.
[29] Börner HG, Beers K, Matyjaszewski K, Sheiko SS, Möller M. Macromolecules 2001;34:4375.
[30] Cates ME, Candau SJ. J Phys: Condens Matter 1990;2:6869.
[31] Munk P, Ramireddy C, Tian M, Webber SE, Prochazka K, Tuzar Z. Makromol Chem, Macromol Symp 1992;58:195.
[32] Moffitt M, Khougaz K, Eisenberg A. Acc Chem Res 1996;29:95.
[33] Wang XS, Winnik MA, Manners I. Macromol Rapid Commun 2002;23:210.
[34] Tsubaki K, Ishizu K. Polymer 2001;42:8387.
[35] Beers KL, Boo S, Gaynor SG, Matyjaszewski K. Macromolecules 1999;32:5772.
[36] Mori H, Wakisaka O, Hirao A, Nakahama S. Macromol Chem Phys 1994;195:3213.
[37] Breiner T, Schmidt HW, Müller AHE. e-Polymers 2002;22. Paper No. 22.
[38] Burguiere C, Pascual S, Bui C, Vairon JP, Charleux B, Davis KA, Matyjaszewski K, Betremieux I. Macromolecules 2001;34:4439.
[39] Provencher SW. Comput Phys Commun 1982;27:229.